J. Phys. B: At. Mol. Opt. Phys. **30** (1997) 3611–3626. Printed in the UK PII: S0953-4075(97)82628-4

Electron impact excitation and ionization of laser-excited sodium atoms Na*(7d)

J Nienhaus†, O I Zatsarinny‡, A Dorn† and W Mehlhorn†

† Fakultät für Physik, Universität Freiburg, 79104 Freiburg, Germany

‡ Institute of Electron Physics, Academy of Science, Uzhgorod 294016, Ukraine

Received 17 March 1997

Abstract. We have investigated the ejected-electron spectrum following impact excitation and ionization of laser-excited Na*(nl) atoms by 1.5 keV electrons. By means of two-laser excitation $3s \rightarrow 3p_{3/2} \rightarrow 7d$ and subsequent cascading transitions about 8% (4%) of the target atoms were in excited states with $n > 3$ (7d). The experimental ejected-electron spectrum due to the decay of Auger and autoionization states of laser-excited atoms Na*(nl) with $n = 4$–7 has been fully interpreted by comprehensive calculations of the energies, cross sections and decay probabilities of the corresponding states. The various processes contributing to the ejected-electron spectrum are with decreasing magnitude: 2s ionization leading to $2s2p^6nl$ Auger states, $2p \rightarrow 3s$ excitation leading to $2p^53s(^1P)nl$ autoionization states and $2s \rightarrow 3l'$ excitation leading to $2s2p^63l'(^1L)nl$ autoionization states.

1. Introduction

The method of inner-shell excitation or ionization by photon or electron impact of laser-excited atoms allows us to excite well defined highly excited states which are out of reach by photon or electron impact on the ground-state atom. The investigation of these states via their decay by means of Auger or autoionization electron spectrometry (AES) or photon spectroscopy yields new information on the structure and the dynamics of atoms. Most of the AES investigations on laser-excited atoms were performed in connection with photo-excitation by using synchrotron radiation (Wuilleumier *et al* 1988, Nunnemann *et al* 1985). Recently, we performed AES experiments after electron impact excitation and ionization of laser-excited Na*(nl) with $nl = 3p, 4d, 5s$ and we obtained information on energies, cross sections, alignment and relative decay rates of many new states (Dorn *et al* 1994, 1995a, b, 1997). In particular, we studied the excitation and non-radiative decay of Auger states $2s2p^6nl\,^{1,3}L$ of Na with $nl = 3p, 4p, 5p, 4d, 5d, 6d, 5s, 6s, 7s$ (Dorn *et al* 1995a, b, Grum-Grzhimailo and Dorn 1995). These investigations were a first step in a study of the dynamical correlation in the decay of Auger states $2s2p^6nl\,^{1,3}L$ of Na. These Auger states can be prepared by two-step laser excitation $3s \rightarrow 3p_{3/2} \rightarrow nl$ of Na atoms and simultaneous 2s ionization by electron impact. They decay either by non-radiative or radiative transitions

$$Na^{+*}(2s2p^6nl\,^{1,3}L) \rightarrow Na^{2+}(2s^22p^5\,^2P) + e_A^- \quad (1a)$$

$$\rightarrow Na^{+*}(2s^22p^5nl\,^{1,3}L') + \gamma. \quad (1b)$$

The probability for non-radiative decay depends decisively on the excited nl electron via the Coulomb matrix element $\langle 2s\epsilon_A l_A|\frac{1}{r_{12}}|2pnl\rangle$, while the matrix element $\langle 2s|r|2p\rangle$ for the radiative decay is practically independent of nl. In other words, the non-radiative decay is

0953-4075/97/163611+16$19.50

governed by the dynamical correlation of the electron pair 2pnl. By laser exciting the 3s electron of Na to different nl, the change in the dynamical correlation can be studied via the change of the branching ratio between the decay channels (1a) and (1b). For example, for $nl = 7$d the partial width due to radiative decay 2p $\rightarrow$ 2s is 1.7×10^{-2} meV compared with the partial widths due to Auger decay of 2.0 and 4.5 meV for 2s2p^{6}7d ^{1}D and ^{3}D (Zatsarinny 1995), respectively. Because the probability for Auger decay is proportional to n^{-3}, one needs an excitation to $n = 10 \ldots 15$ in order to obtain fluorescence yields between 1 and 10%.

In order to test the feasibility of such an investigation we studied the Auger and autoionization spectra for electron impact on laser-excited Na*(7d), the results of which are presented in this paper. This paper is organized as follows. In section 2 we briefly describe the apparatus and experimental procedure. In section 3 experimental spectra are presented. Section 4 gives an account of the method of our calculation of the energies, cross sections and decay probabilities of Auger and autoionizing states. In section 5 we compare and discuss the experimental and theoretical results. Finally, section 6 concludes the paper.

2. Apparatus and experimental procedure

The experimental set-up has previously been described in detail (Dorn *et al* 1994, 1995a, 1997), therefore only a summary of the basic parameters is given here. The laser beams (along the y-axis) and the 1.5 keV electron beam (along the z-axis) cross the atomic sodium beam (x-axis). The Na atoms are emanating from an oven operating at a temperature of about 575 K which is considerably lower than in our previous experiments (Dorn *et al* 1995a, b, 1997).

The Na atoms are laser excited in two steps: 3s $\rightarrow$ 3p$_{3/2}$ $\rightarrow$ 7d. The relative density of Na(3s) in the target volume is determined as in previous experiments (Dorn *et al* 1995a, 1997). The relative density of Na*(3p$_{3/2}$) is determined in an analogous way: the Auger states 2s2p^{6}3p ^{1,3}P can be produced by 2s ionization of ground-state atoms Na(3s) (via a conjugate shake-up transition) or laser-excited Na*(3p). The decay of these Auger states into 2s^{2}2p^5 ^{2}P + e_A^- gives rise to a four-component structure between 22 and 23 eV. From the intensities of this structure measured in previous works (Dorn *et al* 1995a) without laser excitation (100% Na(3s)) and with laser excitation 3s $\rightarrow$ 3p$_{3/2}$ with known relative densities n_{rel}(Na(3s)) and n_{rel}(Na(3p$_{3/2}$)) the following relation for the intensity can be found

$$I_{\mathrm{Auger}}(2s2p^6 3p) = C\{n_{\mathrm{rel}}(\mathrm{Na}(3p_{3/2})) + 0.105 n_{\mathrm{rel}}(\mathrm{Na}(3s))\}. \qquad (2)$$

The constant C depends on the absolute density of Na atoms and the energy and intensity of the incident electrons. The determination of n_{rel}(Na(3p$_{3/2}$)) is now a matter of two steps. In the first step with laser excitation 3s $\rightarrow$ 3p$_{3/2}$ the quantities n_{rel}(Na(3s)), n_{rel}(Na(3p$_{3/2}$)) = 1 $-$ n_{rel}(Na(3s)) and I_{Auger} are measured and C can be evaluated by equation (2). In the second step with two-laser excitation 3s $\rightarrow$ 3p$_{3/2}$ $\rightarrow$ 7d the quantities n_{rel}(Na(3s)) and I_{Auger} are measured, and with the now known value C the relative density n_{rel}(Na(3p$_{3/2}$)) is evaluated by using equation (2). This procedure yielded the relative densities n_{rel}(Na(3s)) = 0.60 and n_{rel}(Na(3p$_{3/2}$)) = 0.32. The relative densities of Na in other states reached by the radiative decay of the laser-pumped 7d level were calculated by integrating the rate equations taking into account the Doppler and the power broadening of the states. The partitioning of the remaining 8% of atoms in higher states than 3p$_{3/2}$ is as

follows:

$$\begin{aligned} &7d_{5/2}(0.35),\ 7d_{3/2}(0.17),\ 7p_{3/2}(0.13),\ 7p_{1/2}(0.05),\\ &6p_{3/2}(0.09),\ 6p_{1/2}(0.04),\ 6s_{1/2}(0.01),\\ &5p_{3/2}(0.06),\ 5p_{1/2}(0.02),\ 5s_{1/2}(0.01),\\ &4p_{3/2}(0.04),\ 4p_{1/2}(0.02),\ 4s_{1/2}(0.02). \end{aligned} \tag{3}$$

Primary electrons with 1.5 keV energy are used for inner-shell excitation or ionization. The Auger and autoionization electrons are energy selected by means of a sector CMA with an energy resolution of 108 meV at 30 eV and are detected by a position-sensitive detector. The electrons are measured at the magic angle of $\theta_m = 125.3^\circ$.

When exciting the atoms to 7d by the second laser, we observed a very strong effect in the electron spectrum: the line positions are shifted to lower energies and the line widths are dramatically broadened. These effects are due to the Penning ionization in collisions between excited Na atoms (Wuilleumier *et al* 1988, Dengel *et al* 1993)

$$\mathrm{Na}^*(nl) + \mathrm{Na}^*(3p) \rightarrow \mathrm{Na}(3s) + \mathrm{Na}^+ + \mathrm{e}^-(2.11\ \mathrm{eV} - E_{nl}) \tag{4}$$

where E_{nl} is the binding energy of $\mathrm{Na}^*(nl)$. The electrons escape from the atomic beam and a positive charge density is left in the target volume. The cross section for Penning ionization is about 10 times the geometrical cross section, $\sigma_P \simeq 10\pi(r_{nl}+r_{3p})^2$ (Wuilleumier *et al* 1988, Dengel *et al* 1993, Olson 1979), which scales roughly with $(n^2+3^2)^2$. Therefore the Penning cross section for $n = 7$ in (4) is about a factor of 5.4 larger than in the previous experiments (Dorn *et al* 1995a, b, 1997). To avoid the shift and the broadening of electron lines we had to reduce the Na target density to about 1×10^{11} atoms/cm^3. This reduction of target density caused an equivalent reduction of the intensity of the ejected electrons.

3. Experimental spectra

In figure 1(*a*) the measured electron spectra with laser excitation $3s \rightarrow 3p_{3/2}$ (broken curve) and with two-laser excitation $3s \rightarrow 3p_{3/2} \rightarrow 7d$ (full curve) are shown. The two line groups between 29.5 and 30.0 eV and between 30.5 and 31.0 eV are due to the decay of $\mathrm{Na}^{**}(2p^5 3s(^3P)3p\,^2L)$ and $\mathrm{Na}^{**}(2p^5 3s(^{1,3}P)4s\,^2P)$, respectively (Dorn *et al* 1997). They have their origin mainly in the electron impact of ground-state atoms Na(3s) and laser-excited atoms $\mathrm{Na}^*(3p_{3/2})$. For electron energies above 31.2 eV the two spectra of figure 1(*a*) show differences due to laser-excited states higher than $3p_{3/2}$. To examine these differences in more detail we subtract the contributions due to electron impact excitation of Na(3s) and $\mathrm{Na}^*(3p_{3/2})$ from the full curve spectrum obtained with two-step laser excitation. For this reason we construct from the known electron spectra for electron impact on Na(3s) and on $\mathrm{Na}^*(3p_{3/2})$ (Dorn *et al* 1995b, 1997) a spectrum for a mixed target Na(3s) and $\mathrm{Na}^*(3p_{3/2})$ with relative densities in proportion to 0.60:0.32. This spectrum is normalized in intensity to the lines between 29.5 and 30.0 eV of the full curve spectrum of figure 1(*a*) and then subtracted from this spectrum. The resulting electron spectrum is plotted in figure 1(*b*). It is due to electron impact ionization and excitation of a mixture of $\mathrm{Na}^*(nl)$ with the relative densities given in (3). For a quantitative interpretation of this spectrum we need theoretical values for the excitation and ionization cross sections and decay probabilities of the various Auger and autoionization states.

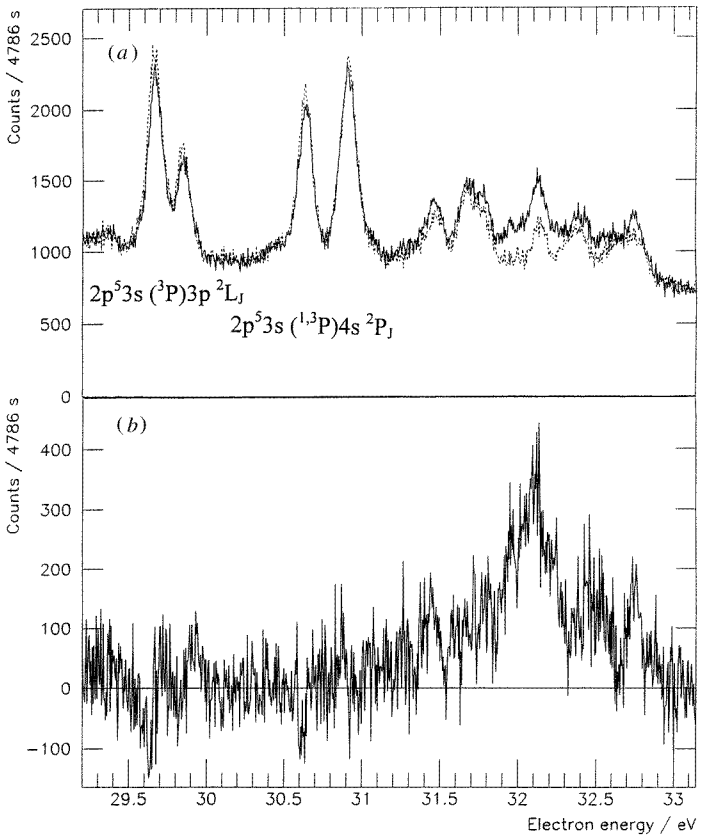

Figure 1. Ejected-electron spectra. (*a*) The ejected-electron spectra after electron impact at 1.5 keV on one-step 3s → $3p_{3/2}$ (broken curve) and two-step 3s → $3p_{3/2}$ → 7d (full curve) laser-excited Na. (*b*) The ejected-electron spectrum without contributions of Na(3s) and $Na^*(3p_{3/2})$ (see text for details).

4. Method of calculation

Electron spectra of atoms with several open shells are complex and cause difficulties in their interpretation. Even for atoms with a simple shell structure, as in the case of Na, the number of possible decay channels may be large and increases further by an essential fine-structure splitting. This complicates the experimental identification of the Auger and autoionization lines, and the unique identification of the corresponding states needs a direct comparison of experimental and theoretical spectra. In this case the calculations have to include not only the positions of the states but also their excitation cross sections and their decay rates into different channels.

The fact that not only one single but several processes produce lines in the ejected-electron spectrum of sodium makes the theoretical interpretation of the spectrum more complex. In addition, the electron emission lines, originating from Auger and autoionizing states of both Na^+ and Na, lie in the same energy region. For example, the electron lines in the considered energy region of 29–33 eV after 1.5 keV electron impact on $2s^2 2p^6 nl$ can result from the following processes: 2p → 3s excitation leading to $2p^5 3snl$ autoionizing

states, $2s \rightarrow 3l'$ excitation leading to $2s2p^6 3l'nl$ states, and 2s ionization leading to $2s2p^6 nl$ Auger states. In the theoretical analysis we include all these processes. Details of our calculation scheme have been outlined in our previous works (Zatsarinny and Bandurina 1993, Zatsarinny 1995, Dorn *et al* 1997). Therefore, we briefly summarize only a few essential points and outline some new features. These features are connected with the fact that for the interpretation of the present measurements we have to include the states with large principal quantum numbers of the outer electron (up to $n = 12$). It leads not only to an extension of our previous calculations (Dorn *et al* 1997), but due to the multiplet and fine-structure splittings of excitation thresholds for the $2p^5 3snl$ and $2s2p^6 3l'nl$ autoionizing series, many new decay channels appear which considerably complicate the calculations.

4.1. 2p → 3s excitation

The general scheme for this process and its subsequent decay is as follows

$$\begin{aligned} e^- + Na^*(2p^6 nl_j) \rightarrow e^- + Na^{**}(2p^5 n_1 l_1 (L'S'J') n_2 l_2 LSJ) \\ \hookrightarrow \quad Na^+(2p^6) + e^-_{A1} \\ \hookrightarrow \quad Na^+(2p^5 3s\,{}^3P_{0,1,2}) + e^-_{A2}. \end{aligned} \tag{5}$$

Wavefunctions for the $2p^5 n_1 l_1 n_2 l_2$ autoionizing states have been obtained in the intermediate coupling fixed-core CI approximation, where the many-configurational expansion has the form

$$\Psi^J = \sum_{i=\{n_1 l_1; n_2 l_2; L'S'; LS\}} C_i \Phi_i^{LS}(1s^2 2s^2 2p^5 n_1 l_1 (L'S') n_2 l_2) \tag{6}$$

and core–valence correlation is included through the model core-polarized potential. The details of the calculation scheme are given by Zatsarinny and Bandurina (1993). To investigate the states $2p^5 3snl$ with n up to 12, the configuration basis in (6) has been considerably extended for the present calculations and included up to 1200 basis functions $2p^5 n_1 l_1 n_2 l_2$ ($n_1 \leqslant 5$, $n_2 \leqslant 15$, $l_1, l_2 \leqslant 4$). An important detail of the present calculations concerns the autoionization states lying at energies between the $2p^5 3s\,{}^3P_{0,1,2}$ and ${}^1P_1$ excitation thresholds and higher. To have the same orthogonal set of one-particle radial orbitals for all states under consideration, the radial orbitals for outer electrons ($nl = n_1 l_1, n_2 l_2$) have been obtained from Hartree–Fock (HF) calculations for the $2p^5 nl$ states of Na^+. In this case, due to the finiteness of the basis, the CI method gives, for each series of autoionizing states under consideration, three additional so-called 'non-physical' levels (Robaux 1988), one of these lies closely below the excitation threshold, while the others lie above the threshold. The former level represents the rest of the infinite number of bound series levels, while the latter two levels represent the corresponding continuum. Although this is a very rough approximation it leads to a considerable improvement of calculated level parameters (Robaux 1988). But, in the energy region close to the excitation threshold one has to take into account one unpleasant property of these 'non-physical' levels: on increasing the basis their energies and configuration expansions change chaotically and do not converge to any fixed value. Therefore, these 'non-physical' levels (e.g. for $3s(^3P)nl$ series) may interact chaotically with the physical levels of higher series (e.g. with $3s(^1P)nl$ series) which may lead to inaccuracies for the latter levels. In this case the 'non-physical' levels should be excluded, for example, by a two-step diagonalization of the Hamiltonian (Zatsarinny *et al* 1991). In a first step the submatrix associated only with the series converging to the same threshold is diagonalized. In a second step a new basis is built

from the obtained wavefunctions excluding levels with 'positive' energies, i.e. the 'non-physical' levels. Such a procedure is done in the present calculations for each energy region between and above the $2p^5 3s\,{}^3P_{0,1,2}$ and ${}^1P_1$ excitation thresholds which makes the calculation much more cumbersome.

The autoionizing states in this energy region have several decay channels (see (5)) where also the fine-structure splitting of the residual ion terms has to be accounted for. Therefore, the continuum wavefunctions which one needs for the computation of autoionization widths have been calculated in the jK-coupling scheme by using the program IMPACT (Crees *et al* 1979) with full accounting for the coupling of different decay channels. Up to 10 channels have to be considered simultaneously. In general, the decay into the excited states of the residual ion was found to be dominant.

The electron impact 2p excitation cross sections of the $2p^5 3snl$ states have been calculated in the first Born approximation with full accounting for the relaxation of the outer electron nl during the 2p excitation process. The computational details are given by Dorn *et al* (1997). To cover all excitation modes under consideration the calculations of cross sections were carried out for the 617 autoionizing states $2p^5 3snl$ excited from 25 initial atomic states $2p^6 3s_{1/2}, 3p_{1/2,3/2}, 3d_{3/2,5/2}, \ldots, 7d_{3/2,5/2}$. The intermediate coupling scheme for the high-lying autoionization states was found to be very close to the pure jK coupling ($2p^5 3s({}^{1,3}P)nl[K]J$) with the intermediate spin being a good quantum number. Therefore, only the $2p^5 3s({}^1P)nl$ states are excited effectively at high impact energies, and the corresponding cross sections were found to be about 10^{-18} cm^2 at the incident electron energy $E = 1.5$ keV. As an example, table 1 presents the energies, widths, branching ratios to the ionic ground state and excitation cross sections for the $2p^5 3s({}^1P_1)np$ (table 1(*a*)) and $2p^5 3s({}^1P_1)nd$ (table 1(*b*)) series. The possibility of radiative decay of the autoionizing states was also taken into account in the calculations of the branching ratios. It is seen from table 1 that the autoionization states above the thresholds $2p^5 3s\,{}^3P$ decay dominantly into the excited states $2p^5 3s\,{}^3P_{0,1,2}$ of the residual ion and do not contribute to electron spectra in the energy region of interest, 29–32 eV. As a result, only states with configurations $2p^5 3s({}^1P_1)4d, 5p, 6s, 5d$ and 6p may give rise to the lines in the ejected-electron spectra at high energies (figure 1(*b*)), whereas the states with larger n values produce only electrons with energies smaller than 1 eV. Therefore, although the 2p excitation is most effective for producing autoionization states, it leads, at present laser-excitation mode, to electron lines with intensities smaller than the lines due to 2s ionization.

4.2. 2s ionization

The 2s ionization cross section has been evaluated in the sudden approximation as a two-step process: pure 2s ionization plus shake-up of an outer electron. The general scheme for this process and for the subsequent decay is as follows:

$$e^- + Na^*(2s^2 2p^6 nl_j) \rightarrow 2e^- + Na^{+*}(2s2p^6 n'lLSJ)$$
$$\hookrightarrow \quad Na^{2+}(2p^5\,{}^2P_{1/2}) + e_A^-(l \pm 1) \qquad (7a)$$
$$\hookrightarrow \quad Na^{2+}(2p^5\,{}^2P_{3/2}) + e_A^-(l \pm 1). \qquad (7b)$$

The total effective cross section for the separate Auger lines (7*a*) and (7*b*) contains four factors. The total 2s-ionization probability $\sigma(2s\ \text{ion})$, its dependence from quantum numbers of the initial nl_j state and the Auger state $K(nl_j \rightarrow LSJ)$, the shake probability of the outer electron $|\langle nl|n'l\rangle|^2$, and the partial decay probability into the separate channels (7*a*) or (7*b*) $A(LSJ \rightarrow {}^2P_{1/2,3/2})$, i.e.

$$\sigma^{2s} = \sigma(2s\ \text{ion}) \times K(nl_j \rightarrow LSJ) \times |\langle nl|n'l\rangle|^2 \times A(LSJ \rightarrow {}^2P_{1/2,3/2}). \qquad (8)$$

Table 1. Energies E (relative to $2p^6$), widths G, branching ratios w to $2p^6$, and excitation cross sections (in barn) of the $2p^5 3s(^1P_1)nl[K]J$ autoionizing states in Na from the initial (*a*) $2p^6 6p$, 7p and (*b*) $2p^6 6d$, 7d atomic states for 1.5 keV electron impact.

						Excitation cross sections			
Configuration	$[K]$	J	E (eV)	G (meV)	w (%)	$6p_{1/2}$	$6p_{3/2}$	$7p_{1/2}$	$7p_{3/2}$
(*a*)									
$3s(^1P_1)4p$	[2]	5/2	31.668	0.318E + 00	99.4	0	4 524	0	2 085
$3s(^1P_1)4p$	[0]	1/2	31.685	0.418E + 01	100.0	1 464	678	670	310
$3s(^1P_1)4p$	[2]	3/2	31.685	0.199E + 00	99.0	4 963	260	2 268	120
$3s(^1P_1)4p$	[1]	3/2	31.715	0.197E + 00	99.1	500	2 184	222	983
$3s(^1P_1)4p$	[1]	1/2	31.728	0.230E − 01	92.8	1 097	622	493	278
$3s(^1P_1)5p$	[2]	5/2	32.428	0.744E − 01	97.3	0	17 020	0	4 729
$3s(^1P_1)5p$	[2]	3/2	32.431	0.644E − 01	97.4	14 972	281	4 747	153
$3s(^1P_1)5p$	[0]	1/2	32.436	0.770E + 00	99.8	6 785	769	1 958	236
$3s(^1P_1)5p$	[1]	3/2	32.437	0.606E − 03	27.4	3 640	7 227	883	1 601
$3s(^1P_1)5p$	[1]	1/2	32.439	0.386E + 00	99.6	761	3 227	108	887
$3s(^1P_1)6p$	[2]	5/2	32.763	0.359E − 01	94.5	0	380 720	0	15 537
$3s(^1P_1)6p$	[2]	3/2	32.764	0.240E − 01	94.4	341 701	163	13 706	4
$3s(^1P_1)6p$	[0]	1/2	32.767	0.471E + 00	99.7	122 282	14 042	4 091	606
$3s(^1P_1)6p$	[1]	3/2	32.770	0.671E − 02	81.4	3	193 234	3	6 348
$3s(^1P_1)6p$	[1]	1/2	32.772	0.757E − 01	98.1	134 592	27 962	4 034	877
Threshold $3s\ ^3P_2$		—	32.847	—	—	—	—	—	—
$3s(^1P_1)7p$	[2]	5/2	32.940	0.654E + 00	7.6	0	37 994	0	389 228
$3s(^1P_1)7p$	[2]	3/2	32.941	0.337E + 00	12.5	47 003	603	509 656	6 085
$3s(^1P_1)7p$	[1]	3/2	32.943	0.629E + 00	0.5	890	19 521	13 237	262 176
$3s(^1P_1)7p$	[0]	1/2	32.943	0.556E + 00	2.7	7 899	6 350	101 663	83 018
$3s(^1P_1)7p$	[1]	1/2	32.944	0.369E + 00	0.0	11 497	3 589	167 634	51 303
Threshold $3s\ ^3P_0$		—	33.015	—	—	—	—	—	—
$3s(^1P_1)8p$	[2]	5/2	33.045	0.294E + 00	4.5	0	6 520	0	36 930
$3s(^1P_1)8p$	[2]	3/2	33.046	0.121E + 00	9.4	8 022	231	44 862	1 266
$3s(^1P_1)8p$	[1]	3/2	33.047	0.421E + 00	0.0	360	3 402	2 033	18 524
$3s(^1P_1)8p$	[0]	1/2	33.047	0.219E + 00	17.4	2 078	795	11 264	4 356
$3s(^1P_1)8p$	[1]	1/2	33.048	0.280E + 00	0.0	1 457	1 001	7 886	5 357
$3s(^1P_1)9p$	[2]	5/2	33.113	0.227E + 00	5.0	0	2 422	0	6 351
$3s(^1P_1)9p$	[2]	3/2	33.114	0.101E + 00	9.7	3 037	71	7 917	183
$3s(^1P_1)9p$	[1]	3/2	33.114	0.241E + 00	0.1	97	1 301	260	3 367
$3s(^1P_1)9p$	[0]	1/2	33.114	0.152E + 00	19.3	1 007	183	2 595	476
$3s(^1P_1)9p$	[1]	1/2	33.115	0.164E + 00	0.0	333	495	864	1 271
$3s(^1P_1)10p$	[2]	5/2	33.159	0.111E + 00	7.0	0	1 179	0	2 358
$3s(^1P_1)10p$	[0]	1/2	33.160	0.117E + 00	12.2	0	333	0	658
$3s(^1P_1)10p$	[2]	3/2	33.160	0.451E − 01	15.5	1 426	68	2 838	134
$3s(^1P_1)10p$	[1]	3/2	33.160	0.158E + 00	0.1	105	607	213	1 205
$3s(^1P_1)10p$	[1]	1/2	33.160	0.116E + 00	0.1	659	0	1 306	0
Threshold $3s\ ^1P_1$		—	33.323	—	—	—	—	—	—

All these factors were discussed by Dorn *et al* (1997). The necessary parameters (energies, total and partial decay widths) of the $2s2p^6nl$ Auger states for $n \leqslant 8$ were calculated by

Table 1. (Continued)

						Excitation cross sections			
Configuration	[K]	J	E (eV)	G (meV)	w (%)	$6d_{3/2}$	$6d_{5/2}$	$7d_{3/2}$	$7d_{5/2}$
(*b*)									
$3s(^1P_1)4d$	[1]	3/2	32.363	0.154E + 00	99.6	12	698	0	208
$3s(^1P_1)4d$	[3]	5/2	32.366	0.571E − 02	86.4	1 903	463	517	110
$3s(^1P_1)4d$	[1]	1/2	32.368	0.226E + 00	99.7	268	0	130	0
$3s(^1P_1)4d$	[3]	7/2	32.374	0.286E − 03	17.8	0	1 896	0	690
$3s(^1P_1)4d$	[2]	3/2	32.378	0.269E − 01	94.9	1 550	20	574	2
$3s(^1P_1)4d$	[2]	5/2	32.380	0.416E − 05	0.3	595	1 299	233	477
$3s(^1P_1)5d$	[3]	5/2	32.718	0.425E − 01	96.3	10 033	2 530	6 603	3 548
$3s(^1P_1)5d$	[3]	7/2	32.729	0.613E − 01	97.0	0	11 629	0	511
$3s(^1P_1)5d$	[2]	3/2	32.730	0.163E + 00	98.9	6 744	986	1 149	1 139
$3s(^1P_1)5d$	[2]	5/2	32.734	0.691E − 02	77.7	3 352	5 445	75	706
$3s(^1P_1)5d$	[1]	1/2	32.746	0.511E + 00	99.7	1 965	0	319	0
$3s(^1P_1)5d$	[1]	3/2	32.749	0.127E + 01	99.8	800	2 841	211	338
Threshold $3s\ ^3P_2$		—	32.847	—	—	—	—	—	—
$3s(^1P_1)6d$	[3]	5/2	32.908	0.349E + 01	0.7	280 970	39 922	15 304	2 763
$3s(^1P_1)6d$	[3]	7/2	32.912	0.296E + 02	0.1	0	302 555	0	11 883
$3s(^1P_1)6d$	[2]	3/2	32.917	0.606E + 01	0.3	167 432	55 966	6 447	2 451
$3s(^1P_1)6d$	[2]	5/2	32.919	0.147E + 02	0.0	63 030	210 647	1 653	7 036
$3s(^1P_1)6d$	[1]	3/2	32.925	0.273E + 01	0.0	88 677	121 707	1 998	2 701
$3s(^1P_1)6d$	[1]	1/2	32.925	0.228E + 01	10.4	136 512	0	3 002	0
Threshold $3s\ ^3P_1$		—	32.942	—	—	—	—	—	—
$3s(^1P_1)7d$	[3]	5/2	33.003	0.602E + 01	0.0	38 179	2 068	1 104	130
$3s(^1P_1)7d$	[3]	7/2	33.003	0.105E + 02	0.0	0	37 285	0	825
$3s(^1P_1)7d$	[2]	3/2	33.007	0.255E + 01	2.1	6 916	5 623	232	60
$3s(^1P_1)7d$	[2]	5/2	33.007	0.413E + 01	0.0	1 455	14 437	1	288
$3s(^1P_1)7d$	[1]	3/2	33.008	0.218E + 01	8.2	7 694	2 233	87	6
$3s(^1P_1)7d$	[1]	1/2	33.009	0.165E + 01	0.0	4 979	0	14	0
Threshold $3s\ ^3P_0$		—	33.015	—	—	—	—	—	—
$3s(^1P_1)8d$	[3]	7/2	33.059	0.638E + 02	0.1	0	44 306	0	269 764
$3s(^1P_1)8d$	[3]	5/2	33.060	0.386E + 02	0.1	42 950	2 643	302 394	22 024
$3s(^1P_1)8d$	[2]	3/2	33.068	0.232E + 02	2.1	16 779	4 576	163 885	51 229
$3s(^1P_1)8d$	[2]	5/2	33.068	0.267E + 02	0.0	3 216	21 212	29 033	216 083
$3s(^1P_1)8d$	[1]	3/2	33.075	0.685E + 01	9.2	4 994	6 823	75 526	115 137
$3s(^1P_1)8d$	[1]	1/2	33.075	0.599E + 01	0.1	7 299	0	124 541	0
$3s(^1P_1)9d$	[1]	3/2	33.156	0.685E − 01	0.1	6	47	89	2 072
$3s(^1P_1)9d$	[3]	7/2	33.156	0.602E + 00	0.2	0	144	0	3 192
$3s(^1P_1)9d$	[2]	5/2	33.156	0.246E + 00	0.1	48	67	1 309	1 975
$3s(^1P_1)9d$	[3]	5/2	33.156	0.189E + 00	0.4	87	28	2 794	952
$3s(^1P_1)9d$	[2]	3/2	33.157	0.994E − 01	0.2	86	1	3 003	130
$3s(^1P_1)9d$	[1]	1/2	33.157	0.353E − 02	0.0	36	0	1 814	0
Threshold $3s\ ^1P_1$		—	33.323	—	—	—	—	—	—

Zatsarinny (1995) and this calculation was extended in the present work for states up to $n = 12$ (the results are given in table 2). The main difference from the previous calculations by Dorn *et al* (1997) is due to the shake factor. For high-lying states with large principal

Table 2. Energies (relative to the ground state of Na), total decay widths and partial decay widths of Auger states $2s2p^6nl$ for $n = 8$–12 and $l = 0, 1, 2$.

No	State	Energy (eV)	Total width (meV)	Partial widths (meV)	
				$l-1$	$l+1$
8s	3S	84.101	0.533E + 01		0.533E + 01
9s		84.358	0.376E + 01		0.376E + 01
10s		84.538	0.264E + 01		0.264E + 01
11s		84.667	0.192E + 01		0.192E + 01
12s		84.762	0.144E + 01		0.144E + 01
8s	1S	84.112	0.494E + 01		0.494E + 01
9s		84.370	0.359E + 01		0.359E + 01
10s		84.546	0.252E + 01		0.252E + 01
11s		84.673	0.184E + 01		0.184E + 01
12s		84.767	0.138E + 01		0.138E + 01
8p	3P	84.201	0.884E + 00	0.846E + 00	0.494E − 01
9p		84.430	0.603E + 00	0.578E + 00	0.359E − 01
10p		84.589	0.430E + 00	0.412E + 00	0.252E − 01
11p		84.704	0.317E + 00	0.304E + 00	0.184E − 01
12p		84.790	0.241E + 00	0.231E + 00	0.138E − 01
8p	1P	84.208	0.147E + 01	0.383E − 02	0.147E + 01
9p		84.434	0.100E + 01	0.253E − 02	0.997E + 00
10p		84.592	0.710E + 00	0.177E − 02	0.708E + 00
11p		84.707	0.523E + 00	0.129E − 02	0.521E + 00
12p		84.792	0.396E + 00	0.949E − 03	0.395E + 00
8d	3D	84.350	0.305E + 01	0.253E + 00	0.281E + 01
9d		84.533	0.215E + 01	0.167E + 00	0.198E + 01
10d		84.663	0.157E + 01	0.123E + 00	0.145E + 01
11d		84.759	0.119E + 01	0.924E − 01	0.109E + 01
12d		84.832	0.913E + 00	0.717E − 01	0.841E + 00
8d	1D	84.354	0.132E + 01	0.131E + 00	0.119E + 01
9d		84.535	0.929E + 00	0.927E − 01	0.837E + 00
10d		84.665	0.678E + 00	0.681E − 01	0.610E + 00
11d		84.760	0.510E + 00	0.513E − 01	0.459E + 00
12d		84.833	0.393E + 00	0.398E − 01	0.353E + 00

quantum number n, the shake-up probabilities in the case of 2s ionization of Na were found to be very large and increasing with n. For illustration, figure 2(a) displays the average value of n' for the final-state orbital. It is seen that the value of n' with maximum shake-up probability rises for both increasing n and l, and tends to the prediction obtained in the hydrogenic model (Armen 1996). Figures 2(b)–(d) additionally illustrate how the shake probabilities $nl \rightarrow n'l$ vary for s, p and d electrons into final states with $n' = n$, $n + 1$ and $n + 2$. Some general trends are evident: the probability of pure spectator transition $n' = n$ decreases with increasing n and angular momentum l and then oscillates due to nodal effects (figure 2(b)). The shake-up probabilities and the most probable values of n' depend on n and l (figures 2(c) and (d)). For the s orbital, for example, the most probable value of n' is $n' = n$ for $n = 3, 4$, $n' = n + 1$ for $n = 5, 6$ and $n' = n + 2$ for $n = 7, 8$, whereas for the d orbital the most probable value of n' is $n' = n + 1$ for $n = 3, 4, 5$, $n' = n + 2$ for

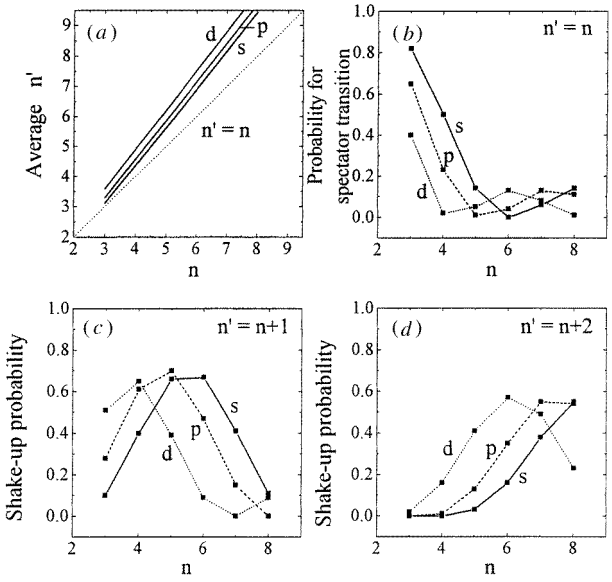

Figure 2. Shake probabilities during 2s ionization, $2s^2 2p^6 nl \rightarrow 2s2p^6 n'l$, of Na. (*a*) Average value of n' of the final states $n'l$ as a function of n and l of the initial state. (*b*) Spectator transition ($n' = n$) probability as a function of n and l of the initial state. (*c*), (*d*) Shake-up transition probabilities $nl \rightarrow n'l$ for s, p and d electrons into final states with $n' = n + 1, n + 2$.

$n = 6, 7$ and $n' = n + 3$ for $n = 8, 9$. In accordance with this result, one can observe the electron lines from the Auger states $2s2p^6 n'l$ with $n' = 8, 9, 10$ in the present experiment when the initial atomic states have $n = 7$ (figure 3). The total shake-down probability was found to be much smaller. It does not exceed 10% and decreases with increasing n. The total shake-off probability can be estimated from the closure relation as $1 - \sum_{n'} |\langle nl|n'l\rangle|^2$. The resulting total shake-off probability does not exceed 6% for all states considered in the present work.

4.3. 2s → 3s, 3p excitation

The general scheme for this process is as follows

$$\begin{aligned} e^- + Na^*(2s^2 2p^6 nl_j) \rightarrow e^- + Na^{**}(2s2p^6 n_1 l_1 (^{1,3}L') n_2 l_2\, LSJ) \\ \hookrightarrow \quad Na^+(2p^6) + e^-_{A1} \\ \hookrightarrow \quad Na^+(2p^5 n_3 l_3\, L_3 S_3 J_3) + e^-_{A2} \\ \hookrightarrow \quad Na^+(2s2p^6 n_3 l_3\, ^{1,3}L'_3) + e^-_{A3}. \end{aligned} \tag{9}$$

Wavefunctions for the $2s2p^6 n_1 l_1 n_2 l_2$ autoionization states have also been obtained in the fixed-core CI approximation, with the many-configurational expansion of the form

$$\Psi^{LS} = \sum_{i=\{n_1 l_1; n_2 l_2; L'S'\}} C_i \Phi_i^{LS}(1s^2 2s2p^6 n_1 l_1 (L'S') n_2 l_2). \tag{10}$$

The calculation scheme is the same as for the $2p^5 n_1 l_1 n_2 l_2$ states (Zatsarinny and Bandurina 1993), the only difference is the structure of the core. As the 2p-shell is closed now, these states are well described in the LS-coupling scheme. For the description of the core polarization in the present calculations we used the same polarization potential as for the

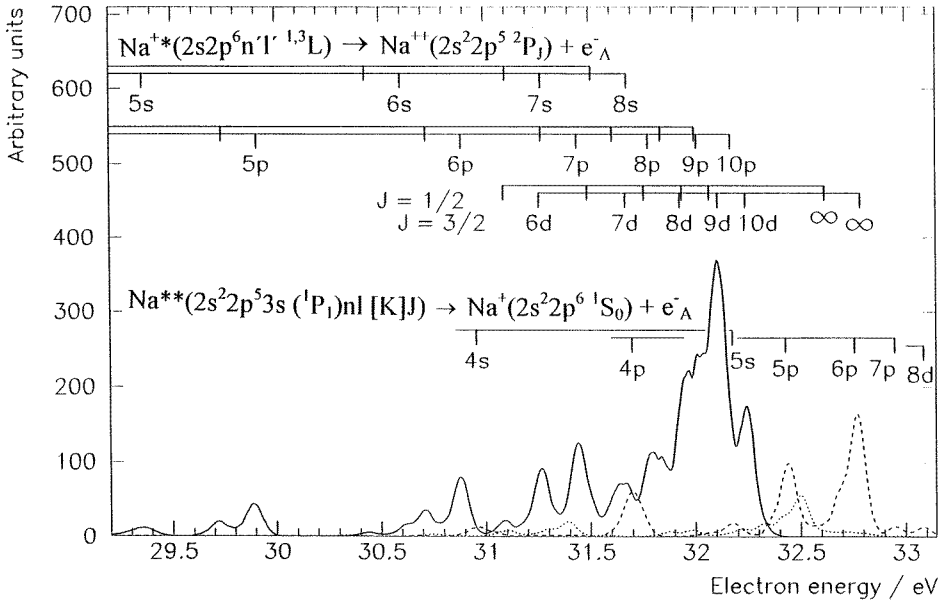

Figure 3. Theoretical spectra representing the three processes discussed in section 4, including the relative occupation numbers (3) of the initial laser-excited states $Na^*(nl)$ and convoluted with the experimental apparatus function. Full curve: Auger electron spectrum due to the decay $Na^{+*}(2s2p^6n'l'^{\,1,3}L) \rightarrow Na^{2+}(2s^22p^{5\,2}P_J) + e^-_A$ after 2s ionization of laser-excited Na. Broken curve: autoionization spectrum due to the decay $Na^{**}(2s^22p^53s(^1P_1)nl[K]J) \rightarrow Na^+(2s^22p^{6\,1}S_0) + e^-_A$ after 2p → 3s excitation of laser-excited Na. Dotted curve: autoionization spectrum after 2s → 3s, 3p excitation of laser-excited Na.

$2s2p^6nl$ Auger states (Zatsarinny 1995). In order to obtain the $2s2p^63l'nl$ states with n up to 12, the configuration basis in (10) contained up to 400 functions with $n_1 \leqslant 5, n_2 \leqslant 15$ and $l_1, l_2 \leqslant 4$. For the states which lie between $2s2p^6nl\,^3L$ and ^1L excitation thresholds the two-step diagonalization procedure was used to exclude the 'non-physical' states as was described in section 4.1. As a result we obtained the energies and wavefunctions for 98 states of the $2s2p^63s(^{1,3}S)nl$ configurations and for 232 states of the $2s2p^63p(^{1,3}P)nl$ configurations. Since the quartet states have very small excitation cross sections at high incident electron energy, only doublet states were considered.

As seen from (9), the $2s2p^63l_1nl$ autoionization states have an infinite number of possible decay channels to the $2p^5n_3l_3$ states of the residual ion. To restrict the number of decay channels which have to be considered, we used the following approximation. It is assumed that the most probable decay for states with large n is the process where the 2p electron, which has the largest overlap with the 2s orbital, makes a transition to this orbital and the least bound electron nl makes a transition to the continuum: $2s2p^63l_1nl \rightarrow 2s^22p^53l_1 + \epsilon l'$. Calculations of partial autoionizing widths for some selected $2s2p^63s(^{1,3}S)nl$ states with inclusion of the $2p^5n_3l_3$ decay channels with $n_3l_3 = 3s, 4s, 5s, 3d, 4d, 5d$ support that the above assumption is valid with high accuracy for states with $n > 5$. We also took into account the fine-structure splitting of the final ion terms and used the many-configuration intermediate coupling wavefunction for the target states. The continuum wavefunctions needed for computation of autoionization widths were calculated in the jK-coupling scheme without accounting for the coupling of different decay channels. The above calculation of autoionization widths included six decay channels for the $2s2p^63snl$ states and 12 decay

Table 3. Energies E (relative to the ground state of Na) and total widths of the $2s2p^63snl$ doublet states of Na. Branching ratios of their decay into final ionic states.

State		E (eV)	G (meV)	Branching ratio (%)					
				$2p^6$	$2p^53s$				$2s2p^63s$
				^1S	$^3P_2$	$^3P_1$	$^3P_0$	$^1P_1$	^3S
$(3s3p)\,^3P$	^2P	66.220	45.371	6	41	12	0	41	
$(3s3p)\,^1P$	^2P	67.957	22.540	17	17	3	3	60	
$(3s3d)\,^3D$	^2D	69.066	9.273	0	62	12	1	24	
$3s(^1S)4s$	^2S	68.938	41.471	1	24	15	5	55	
$(3s3d)\,^1D$	^2D	70.041	3.670	3	17	9	1	71	
$3s(^1S)4p$	^2P	69.680	8.913	18	1	2	3	77	
$3s(^1S)5s$	^2S	70.164	16.183	2	20	11	4	63	
$3s(^1S)4d$	^2D	70.811	1.852	4	2	2	0	92	
$3s(^1S)5p$	^2P	70.437	3.600	19	6	1	0	74	
$3s(^1S)6s$	^2S	70.646	7.960	2	24	14	5	56	
$3s(^1S)6p$	^2P	70.773	1.927	17	1	2	2	78	
$3s(^1S)5d$	^2D	70.803	0.636	0	57	20	2	20	
$3s(^1S)7s$	^2S	70.887	6.266	2	20	11	4	63	
$3s(^1S)7p$	^2P	70.961	1.117	17	6	2	1	75	
$3s(^1S)6d$	^2D	70.963	0.549	2	31	13	1	53	
$2s2p^63s\,^3S$ threshold									
$3s(^1S)8s$	^2S	71.028	7.520	3	14	6	2	69	5
$3s(^1S)8p$	^2P	71.047	0.671	17	2	3	2	72	5
$3s(^1S)7d$	^2D	71.076	23.907	0	0	0	0	1	98
$3s(^1S)9s$	^2S	71.123	7.391	2	0	1	0	19	78
$3s(^1S)8d$	^2D	71.144	13.900	0	0	0	0	1	98
$3s(^1S)9p$	^2P	71.144	0.466	15	2	3	2	74	5
$3s(^1S)9d$	^2D	71.198	13.711	0	0	0	0	2	98

channels for the $2s2p^63pnl$ states. Note, that the decay of the $2s2p^63l_1nl$ states into different $2p^5nl\,^{1,3}L_J$ channels gives rise to electron peaks with an energy separation which is larger than the experimental energy resolution. Therefore, it is important to take into account the detailed information about branching ratios into different decay channels for a careful interpretation of the experimental electron spectrum. It also should be noted, that the effects of relaxation during autoionization was found to be very large and that this relaxation has been taken into account in full measure by using the program of Zatsarinny (1996) for the computation of the autoionization matrix elements in the case of non-orthogonal orbitals.

As an example, table 3 presents the energies, widths and branching ratios into the ground state and excited states for the $2s2p^63s(^1S)nl\,^2L$ series. We see that the dominant decay channel is into the $2p^53s\,^1P_1$ state. Above the $2s2p^63s\,^3S$ threshold the S and D autoionizing states decay dominantly into the $2s2p^63s\,^3S$ state of the residual ion, whereas P states decay dominantly into the $2p^53s\,^1P_1$ state. For the P states the decay into the ground state of Na^+ is also important. In the case of the $2s2p^63p(^1P)nl\,^2L$ states, the dominant decay channels are into $2p^53p\,^1P_1$ and $^1S_0$ states, while the decay to the ground state of Na^+ is also important for the S states. Above the $2s2p^63p\,^3P$ threshold all states decay almost fully (98%) into this latter ionic state.

The 2s excitation cross sections of the $2s2p^63l_1nl$ states by electron impact have been calculated in the first Born approximation. It was found that the most intense transitions

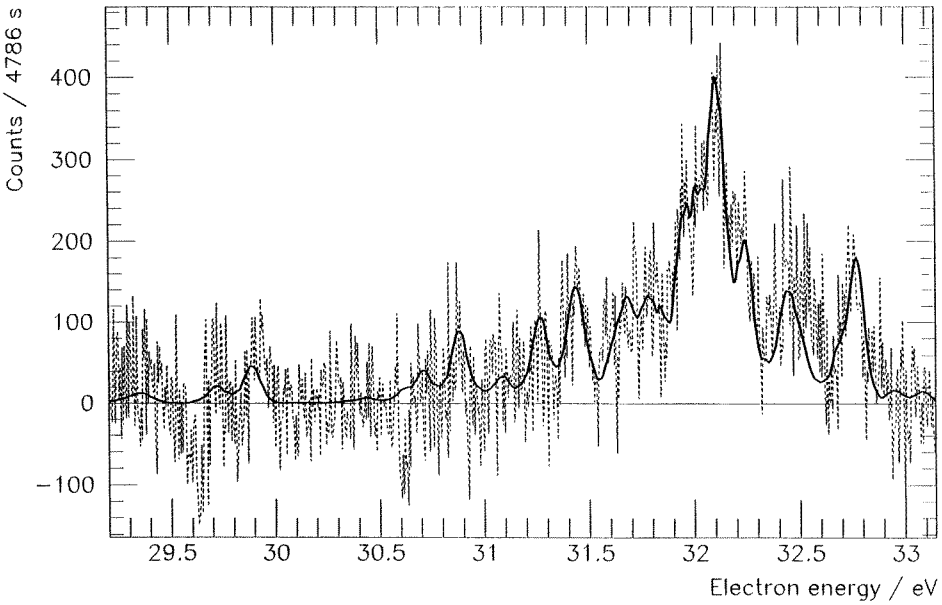

Figure 4. Comparison of experimental and theoretical spectrum. Broken curve: experimental spectrum. Full curve: theoretical spectrum, taken as the sum of the three contributions of figure 3 and scaled in order to obtain a best fit to the experimental spectrum.

are the 2s $\rightarrow$ 3p and 2s $\rightarrow$ 3s excitations; the others, e.g. (2s $\rightarrow$ 3d, 4s), are at least 10 times smaller. Because the intermediate spin is a good quantum number, the most intense transitions were found to the states $2s2p^6 3s(^1S)nl$ and $2s2p^6 3p(^1P)nl$ with cross sections of about 9×10^{-20} and 5×10^{-20} cm^2, respectively, at the incident electron energy $E = 1.5$ keV. Since cross sections for the 2s excitation are much smaller than for the 2p excitation or ionization, the 2s excitation process gives rise to only a small contribution to the ejected-electron spectra under consideration.

With the autoionization state parameters and their effective cross sections at our disposal it becomes possible to predict the ejected-electron spectra observed in the experiment. Theoretical spectra were constructed as a superposition of Lorentzian functions with FWHM equal to the calculated autoionization widths and with intensities being proportional to the effective cross sections. Then, for comparison with the experiment, the theoretical spectra were convoluted with the experimental apparatus function corresponding to an overall energy resolution of 108 meV. In figure 3 we have plotted the various contributions to the ejected-electron spectrum due to 2p $\rightarrow$ 3s excitation (broken curve), 2s ionization (full curve) and 2s $\rightarrow$ 3s, 3p excitation (dotted curve). The sum of all contributions is plotted in figure 4 (full curve) for comparison with the experimental spectrum (broken curve).

5. Discussion

From figure 4 it can be seen that the intensity structures of the experimental electron spectrum are well reproduced by the theoretical spectrum. In the following we will discuss the various processes which contribute to the electron spectrum.

The strongest contribution to the ejected-electron spectrum is from the Auger electrons

of the decay $2s2p^6nl\,^{1,3}L \rightarrow 2s^2 2p^5\,^2P_J + e_A^-$ (full curve in figure 3). The calculated positions of Auger electrons are given as tick marks in the upper part of figure 3. The intensity of the main structure of the electron spectrum between 31.9 and 32.3 eV is due to the Auger decay of $2s2p^6 9d, 10d$ after 2s ionization of $2s^2 2p^6 7d$. This confirms the strong shake-up transitions 7d → 9d and 10d as calculated in section 4.2. Smaller contributions of Auger electrons at lower energies are due to the decay of $2s2p^6 np$ and $2s2p^6 ns$ produced by 2s ionization of excited $Na^*(np, ns)$ via the cascading from $Na^*(7d)$ (see (4)).

The next important process in contributing to the electron spectrum of figure 4 is the $2p^6(^1S) \rightarrow 2p^5 3s(^1P)$ electron impact excitation of laser-excited $Na^*(nl)$ (broken curve in figure 3). In the case of 2p → 3s excitation the shake probabilities of the excited electron nl of levels (4) are small compared with the case of 2s ionization, except for the 7d electron (see tables 1(*a*) and (*b*)). Since the excitation cross section for 2p → 3s excitation is rather independent of the excited electron nl, at least for $n \geqslant 5$, the relative intensities of autoionization electrons of the decay $2p^5 3s(^1P)nl \rightarrow 2p^6 + e_A^-$ reflect the relative densities of laser excited atoms $Na^*(nl)$. This can be easily seen in figure 3 for the atoms excited to 4p, 5p and 6p. In the case of $Na^{**}(2p^5 3s(^1P)7p)$ the energies of the states are already above the threshold $2p^5 3s(^3P_2)$ and the main decay is into this channel with very small ejected-electron energies instead of into the ground state $2p^6(^1S)$ of the ion (see table 1(*a*)). Therefore, the electron intensity at 32.94 eV is correspondingly small. In the case of $Na^*(7d)$ the 2p → 3s excitation leads to a very strong 7d → 8d shake-up (see table 1(*b*)). Again, the states $2p^5 3s(^1P)8d$ autoionize predominantly into the excited ionic states $2p^5 3s(^3P_J)$ with very small energies of the ejected electrons (see table 1(*b*)). Therefore, the autoionization electrons from the decay into $2p^6(^1S_0)$ are barely visible at 33.07 eV.

The very strong and sudden change of the shake probability in the electron impact excitation $2p^6 7d \rightarrow 2p^5 3s(^1P)nd$ is unexpected and needs some more discussion. As seen from table 1(*b*), the cross sections for the $2p^6 7d \rightarrow 2p^5 3s(^1P)nd$ transitions exhibit these pecularities. The largest cross sections are found for the 7d → 8d transition but not for the 7d → 7d one, as it may be expected, because the shake-up probabilities for transitions without changing the effective charge for the outer electron are small. Indeed, the calculations with single-configuration HF wavefunctions for the $2p^5 3snd$ states show that the most intense transition has to be the 7d → 7d one. It will be shown in the following, that the above pecularity is due to the configuration mixing between the $2p^5 3snd$ states and perturber states. The strongest perturbers for the $2p^5 3snd$ series are the $2p^5(3p^2\,^1D)\,^2P$, ^2D and ^2F states. Consider, for example, the interaction of the $2p^5(3p^2\,^1D)\,^2D$ perturber with the $2p^5 3s(^1P)nd\,^2D$ series. Table 4 lists the energies for this series calculated in LS-coupling without inclusion of the interaction with the perturber (energies E_1) and with inclusion of the perturber (energies E_2). We see that without interaction the $3p^2(^1D)\,^2D$ state is between the 6d and 7d levels of the $2p^5 3s(^1P)nd\,^2D$ series. If the interaction is turned on, this state is pushed to above the $2p^5 3s\,^1P_1$ threshold and the energies of the $2p^5 3s(^1P)nd$ states change as well as the corresponding configuration expansions. It is this redistribution of energies and configuration expansion which leads to the drastic change of shake probabilities of the outer electron. For the $2p^6 7d \rightarrow 2p^5 3s(^1P)nd$ transitions the shake probabilities can be approximately estimated as $S = |\sum c_n \langle 7d|nd\rangle|^2$, where c_n are the expansion coefficients for the $3snd$ basis configurations. The values of S, obtained without interaction with the perturber (S_1) and with the perturber (S_2), are compared in table 4. We see that the configuration interaction with the perturber leads to a drastic change of the shake probabilities: without perturber the 7d electron stays in its quantum state (93%) whereas with the perturber the shake-up transition 7d → 8d has the largest probability (69%) followed by the shake-down process 7d → 6d (27%).

Table 4. Energies E_1, E_2 (relative to the ground state of Na) of states of the series $2p^5 3s(^1P)nd\,^2D$ of Na and shake probabilities S_1, S_2 for 7d electron during the $2p^6 7d\,^2D \rightarrow 2p^5 3s(^1P)nd\,^2D$ transition, both calculated without (index 1), respectively with (index 2) inclusion of the perturber $2p^5(3p^2\,^1D)\,^2D$ (see text for details).

Configuration	E_1 (eV)	E_2 (eV)	S_1 (%)	S_2 (%)
$3s(^1P)4d$	37.574	37.504	0.7	0.1
$3s(^1P)5d$	37.890	37.856	0.1	0.3
$3s(^1P)6d$	38.063	38.041	5.0	27.3
$3p^2(^1D)$	38.098			
$3s(^1P)7d$	38.151	36.691	93.0	0.1
$3s(^1P)8d$	38.267	37.504	0.7	69.6
$3s(^1P)9d$	38.309	37.856	0.1	0.1
$3s(^1P_1)$ threshold	38.462			
$3p^2(^1D)$		38.524		

As stated in section 4.3, the $2s \rightarrow 3s, 3p$ excitation by electron impact of laser-excited $Na^*(nl)$ atoms contributes least to the ejected-electron spectrum in the considered energy range (dotted curve in figure 3). Yet, its contribution still improves the agreement between theoretical and experimental spectrum, especially in the energy region around 32.5 eV.

The very good agreement between the theoretical and the experimental spectrum demonstrates that theory is able to correctly calculate all the necessary quantities of Auger and autoionization states produced by 1.5 keV electron impact on laser excited $Na^*(nl)$ to interprete the experimental spectrum. From this one could conclude that also the ejected-electron spectra following electron impact on Na atoms which are laser excited to nd with $n \geqslant 15$ will be quantitatively interpreted by theory. Unfortunately, on the experimental side, the cross section due to Penning ionization will further increase. For example, for laser excitation to 15d the cross section will increase by a factor of 16 compared with the present investigation. In order to keep the present overall energy resolution of 108 meV the target density has to be lowered by a corresponding factor which yields an equivalent reduction of the ejected-electron intensity. This intensity is then already too small to successfully perform an experiment on the dynamical correlation in the decay of the Auger states $2s2p^6nl$, as was pointed out in the introduction.

6. Conclusions

We have investigated the ejected-electron spectrum following impact excitation and ionization of laser-excited $Na^*(nl)$ atoms by 1.5 keV electrons. The laser excitation in two steps $3s \rightarrow 3p_{3/2} \rightarrow 7d$ and the subsequent cascading transitions lead to about 8% of the target atoms being in excited states higher than $3p_{3/2}$ with 52% of these atoms being in the 7d state. The experimental ejected-electron spectrum due to the decay of Auger and autoionization states of laser-excited $Na^*(nl)$ (nl = 7d, 7p, 6p, 6s, 5p, 5s, 4p, 4s) could be quantitatively interpreted by comprehensive calculations of the energies, cross sections and decay probabilities of the corresponding states. It is found that the 2s ionization, leading to Auger states $2s2p^6nl\,^{1,3}L$, contributes strongest to the ejected-electron spectrum in the energy range 29.2–33.1 eV. The impact excitation $2p \rightarrow 3s$ of laser-excited atoms $Na^*(nl)$ leads to large cross sections, but for $n \geqslant 7$ the autoionization states $2p^5 3s(^1P)nl$ lie energetically above the excited ionic state $2p^5 3s(^3P_2)$ and decay predominantly into this channel with very small ejected-electron energies. Therefore, the contribution of $2p \rightarrow 3s$

excitation to the ejected-electron spectrum in the energy region of 29.2–33.1 eV is less important compared with the contribution of the 2s ionization. The excitation $2s \rightarrow 3s, 3p$ in general has smaller cross sections for 1.5 keV electron impact compared with the $2p \rightarrow 3s$ excitation. Therefore, this excitation mode has the least contribution to the intensity of ejected-electron spectrum in the energy range considered in this investigation.

It was also shown that an attempt to study the ejected-electron spectra of Na atoms for laser excitation to even higher Rydberg states, $n = 15 \ldots 20$, would necessarily lead to a reduction of the intensity of ejected electrons to keep the overall energy resolution equal to this work. The reason for this is the strong increase of the Penning ionization cross section with the increase of n leading to a positive charging of the target volume and, as a consequence of this, to a broadening of electron lines. This effect of Penning ionization will therefore prevent an investigation of the dynamical correlation of an electron pair in the transition $2pnl \rightarrow 2s\epsilon_A l_A$, as it was pointed out in the introduction.

Acknowledgments

OIZ acknowledges his stay at the University of Freiburg which was financially supported by the Deutsche Forschungsgemeinschaft via the Sonderforschungsbereich 276. This work is part of the Sonderforschungsbereich 276 'Correlated dynamics of highly excited atomic and molecular states' and was supported by the Deutsche Forschungsgemeinschaft.

References

Armen G B 1996 *J. Phys. B: At. Mol. Opt. Phys.* **29** 677
Crees M A, Seaton M J and Wilson P M H 1979 *Comput. Phys. Commun.* **15** 23
Dengel H, Ruf M-W and Hotop H 1993 *Europhys. Lett.* **23** 567
Dorn A, Nienhaus J, Wetzstein M, Winnewisser C, Eichmann U, Sandner W and Mehlhorn W 1995a *J. Phys. B: At. Mol. Opt. Phys.* **28** L225
Dorn A, Nienhaus J, Wetzstein M, Winnewisser C, Mehlhorn W, Balashov V V, Grum-Grzhimailo A N, Kabachnik N M and Zatsarinny O I 1994 *J. Phys. B: At. Mol. Opt. Phys.* **27** L529
Dorn A, Winnewisser C, Wetzstein M, Nienhaus J, Grum-Grzhimailo A N, Zatsarinny O I and Mehlhorn W 1995b *J. Electron Spectrosc. Relat. Phenom.* **76** 245
Dorn A, Zatsarinny O I and Mehlhorn W 1997 *J. Phys. B: At. Mol. Opt. Phys.* **30** 2975
Grum-Grzhimailo A N and Dorn A 1995 *J. Phys. B: At. Mol. Opt. Phys.* **28** 3197
Nunnemann A, Prescher Th, Richter M, Schmidt M, Sonntag B, Wetzel H E and Zimmermann P 1985 *J. Phys. B: At. Mol. Phys.* **18** L337
Olson R E 1979 *Phys. Rev. Lett.* **43** 126
Robaux O 1988 *J. Phys. B: At. Mol. Opt. Phys.* **21** 3167
Wuilleumier F J, Ederer D L and Piqué J L 1988 *Adv. At. Mol. Phys.* **23** 197
Zatsarinny O I 1995 *J. Phys. B: At. Mol. Opt. Phys.* **28** 4759
——1996 *Comput. Phys. Commun.* **98** 235
Zatsarinny O I and Bandurina L A 1993 *J. Phys. B: At. Mol. Opt. Phys.* **26** 3765
Zatsarinny O I, Lengyel V I and Masalovich E A 1991 *Phys. Rev.* A **44** 7343